

1 Introduction

Governments in emerging economies spend substantial amounts of public money on agricultural policies. A large proportion of such policies are directed towards individual producers (OECD, 2022). While some programs are rigorously evaluated in collaboration with researchers from the program roll-out stage itself (for instance, Boone et al., 2013; Evans et al., 2019), many are not sufficiently evaluated. There are studies that utilize general-purpose survey data to evaluate policies (Abman & Carney, 2020; Agarwala et al., 2022; Shaw et al., 2023) but this is largely a matter of chance, and are often not necessarily evaluating policy outcomes. Further, not all developing countries have systems to collect socio-economic data regularly. Most programs have no reliable pre-implementation data, making them difficult to evaluate.

We provide a solution to this problem by combining the flexibility of pixel-level satellite panel data with a widely used evaluation design to develop a replicable approach. Our solution is constrained only by what satellites can reliably measure. We illustrate our method using remotely sensed indicators of agricultural productivity to evaluate a cash transfer scheme in Telangana, India. The scheme provided substantial transfers to agricultural landowners based on the amount of land they owned. The larger the land, the more the transfer. The wide coverage of the scheme and the large transfers make this policy an ideal program to demonstrate our approach. This study contributes to two broad strands of applied economics research: one, literature on spatial data techniques in economic analysis, and two, literature on agricultural policy evaluation. In the first set of literature, we contribute by demonstrating that pixels can be used units of observation in economic analysis. Economic studies tend to use administrative units (like villages, districts, etc) to conduct analysis (Asher & Novosad, 2020; Deininger et al., 2023). However,

we approach the satellite images as populations of pixels that together represent the relevant regions and then random sample to select a subset of pixels for analysis. The same pixels are observed every month, allowing us to use panel data techniques. In the second set of literature, we engage with studies that analyse agricultural productivity using satellite data (Asher & Novosad, 2020; Blakeslee et al., 2023), as well as contribute to the measurement of productivity change as a result of cash transfer policies (Ambler, de Brauw, et al., 2020; Gazeaud & Stephane, 2023).

To study the effects of a cash transfer programme, we developed a quasi-experimental approach that involved strictly defined treatment and control groups to estimate precise difference-in-differences estimates. Our main outcome of interest is the change in agricultural productivity after the implementation of the cash transfer program. To meet the requirements of experimental designs, we define the treatment and control regions around the Telangana state border. All the owners of land classified as agricultural land inside Telangana received cash transfers. Those on the other side of the border did not receive any comparable transfers during the study period (Shaw et al., 2023). We demonstrate how agricultural policies can be evaluated using remote sensing data in the absence of ground data. Satellite data with high spatial resolution allows us to extract a precise border strip from the treatment and control states. The treatment state is Telangana, where the Rythu Bandhu cash transfer policy was implemented from May 2018 onward, and the control states include its neighbouring states, namely Maharashtra, Karnataka, Andhra Pradesh, and Chhattisgarh. The sample consists of pixels drawn from croplands to exclude forests, other non-agricultural vegetation, and built-up areas. We analyze annual and season-wise impacts on agricultural productivity that were linked to the cash transfer scheme.

Most studies evaluating the impacts of cash transfers have relied on ground-level survey data. In contrast, our study builds upon existing research by utilizing satellite data and remote sensing tools to assess the effects of the Rythu Bandhu cash transfer policy on agricultural productivity in India. Using satellite data offers several advantages over survey data, including eliminating common errors such as survey non-response, bias, sampling errors, and recall issues (Beegle et al., 2012). We rely on and engage with literature that applies remote sensing data to measure economic variables. This literature has developed not in the context of program evaluation but to generate data for unusual research designs (Asher & Novosad, 2020) or to study periods where conventional data is sparse or unavailable (Deininger et al., 2023; Jaafar & Woertz, 2016). For instance, Asher and Novosad, 2020 study the impact of rural road construction on a variety of local economic variables. Variables needed for their analysis were not available at the local level (village in their case). They utilised satellite data to fill these gaps. The other two studies we mentioned were studying agricultural production in regions that were affected by war. Jaafar and Woertz, 2016 looks at how agricultural production levels were maintained to support the war efforts of Islamic State in Syria and Iraq (ISIS). Deininger et al., 2023 assess the effects of the Russia invasion of Ukraine on the agricultural production in Ukraine. They are able to provide a near-real-time assessment of the effects of the combat on area under production and the effects on different farm sizes. Our study develops a policy analysis approach using data similar to these studies, and demonstrates the approach by evaluating a cash transfer-policy's effect on agricultural productivity.

Cash transfer programs designed for agricultural households can improve their welfare in two ways. These two pathways are not necessarily mutually exclusive. One is by enabling consumption expenditure, and two, by providing working capital for

agricultural production, leading to lower debt and/or higher incomes (and again showing up as consumption increases). The present literature on cash transfers primarily focuses on their impact on consumption expenditure, education, and health. Some studies report unintended increases in agricultural productivity, with few studies estimating any intended benefits of cash transfers on agricultural productivity. No studies have looked at the impact of cash transfers on agricultural productivity in the Indian context. We believe that the Indian agricultural context is unique and differs from other contexts ¹, particularly regarding factors such as climate, institutions, landholding size etc.

Cash transfer programs have been implemented in various contexts to increase household welfare. Literature shows that cash transfers help households to increase agricultural production in some cases. Although not intended to increase agricultural production, the evidence from Malawi's social cash transfer programme helped families expand farm production by increasing agricultural assets ownership and time devoted to farm activities(Boone et al., 2013). Experimental evidence from Lesotha shows that cash transfers caused farm production to go up substantially. (Prifti et al., 2019).

Cash transfers can increase agricultural productivity by overcoming credit constraints and due to the increased willingness of risk-averse households to engage in high-risk and high-return farming. Experimental evidence from the Oportunidades cash transfer program in Mexico shows that households consume a portion of the cash transfer while investing the remainder in productive assets.(Gertler et al., 2012) find that households who received cash transfers increased their income by 10% by investing in non-agricultural microenterprises. Additionally, (Todd et al., 2010) find that the Oportunidades helped Mexican households increase their con-

¹Most cash transfer programmes have been evaluated in the Sub-Saharan African context

sumption of food produced on their farms, indicating an increase in agricultural production. The program also led to increased crop production spending, increased livestock ownership, and more land use. (Ambler, De Brauw, et al., 2020) also find that cash transfers combined with the farm management plan increased the gross value output of agriculture by US\$580 relative to the control group. They also found that cash transfers led to increases in livestock and agricultural equipment ownership.

2 Policy Background

The Government of Telangana introduced the Agriculture Investment Support Scheme, also known as Rythu Bandhu, during the kharif season (monsoon crop) of 2018-19. Rythu Bandhu, meaning “friend of the farmer,” is a cash transfer program that provides agricultural landowners Rs 4,000 ($\approx \$58.5$)² per acre per season (subsequently revised to Rs 5,000 or \$73.1). Transfers are made to individuals, not households. A landowner who owns 1 acre of agricultural land would receive Rs 8,000 a year in two instalments. A landowner who owns less or more than 1 acre receives a proportionately smaller or larger transfer. For instance, a farmer with 0.5 acres would receive Rs 4,000 in a year, and another with 10 acres would receive Rs 80,000 per year. Tenant farmers and agricultural labourers who are landless are not covered under this scheme (Ramesh, 2020). The Rythu Bandhu scheme is an unconditional cash transfer. Recipients are free to use the transfers in the way they see fit. There is no need to show the government how the transfer was used.

The program had two objectives: one, to provide working capital to invest in agricultural production, and two, to prevent farmers from taking on too much debt (Minhaz, 2023; Shaw et al., 2023). The transfers are supposed to reach farmers

²Exchange rate used is the 2018 average dollar-rupee rate, which is \$1 = Rs 68.41

before they begin their production cycles in the kharif season (May-June sowing) and in the rabi season (November sowing). The first transfer was provided through cheques, which farmers received starting from 10 May 2018 (Muralidharan et al., 2021). The distribution of cheques took place through village-level meetings under the supervision of State Government Agriculture Officers. Since the second instalment in November-December 2018, transfers began being made directly to beneficiary bank accounts (Muralidharan et al., 2021).

Prior to the launch of Rythu Bandhu, the state government had a three-month rapid Land Records Updation Programme (LRUP) to digitise all land records in the state (Thomas et al., 2020). This programme led to the issuance of land ownership passbooks (called Pattadar Passbooks) to all landowners. The state government now had information about landowners, the type of land owned and the extent of land owned. This allowed them to design Rythu Bandhu in a way that only agricultural landowners were provided transfers. There was no special application procedure, all agricultural landowners received transfers. The favourable reception of this scheme led to similar ones being launched elsewhere. Many state governments (Odisha, West Bengal, Andhra Pradesh, among others) launched new programs. The Union Government of India too launched a nationwide cash transfer for agricultural landowners in early 2019, albeit with smaller transfers.

3 Data

3.1 Inadequacy of on-ground survey data

We choose to exclusively harness satellite data to inform our insights and drive our conclusions. In this section, we expound upon the reasoning that underpins our preference for satellite data over ground survey data.

The National Statistics: Situation Assessment of Agricultural Households conducted a survey in 2013, a time when Telangana had not yet attained the status of a separate state. The next survey was conducted in 2019. Consequently, the survey data from 2013 becomes less relevant to our current analysis due to the substantial changes that have transpired since then. As a result, using this dataset for our study would not yield results that are accurate for our purposes.

Another facet of survey data pertains to the cost of cultivation at the plot level, an annual survey undertaken by the Commission of Agricultural Costs and Prices (CACCP). It is imperative to recognize that this dataset comes with limitations that affect its suitability for our study. The data originates from a three-year panel, where identical plots are surveyed in successive years. Unfortunately, this constrained time frame hinders our capacity to examine pre-treatment trends comprehensively. To attain a thorough grasp of the underlying dynamics, a more extensive temporal span is required. Furthermore, uncertainties surround the representativeness of this dataset, a prerequisite for robust and generalized statistical inferences. Beyond this, the constrained sample size undermines our ability to generate precise estimates, thereby diminishing the statistical validity of our findings. As such, our decision to rely exclusively on satellite data is a well-founded one. This approach empowers us to surmount the inherent limitations of the available survey data sources.

3.2 Data Requirements

We use remote sensing data from different satellites with varying spatial and temporal resolutions to investigate the impact of cash transfers on agricultural productivity. Our two main datasets include Sentinel-2 MSI data and Landsat-8 satellite data. Sentinel-2 is an earth observation system that is part of the Copernicus pro-

gramme, developed by the European Space Agency (ESA).³ This high-resolution satellite has a spatial resolution of 10m and acquires images at each location on the Earth’s surface at 10 a.m. local time, roughly every ten days. In addition to Sentinel-2 data, we use Landsat-8 satellite data, which has a high spatial resolution of 30m and a temporal resolution of 16 days (and captures images at 10 a.m local time).⁴

To verify our findings from Sentinel-2 and Landsat-8 data, we also employ Moderate Resolution Imaging Spectroradiometer (MODIS) satellite images to analyze the impact of changes in spatial resolution on productivity estimates. The MODIS-250 has two sensors, Terra and Aqua, with a spatial resolution of 250m and a temporal resolution of 16 days.

To accurately identify croplands on the ground and ensure that we only measure and analyze light reflected from croplands, we use a dataset from the European Space Agency’s (ESA) World Cover project, which offers a high resolution of 10 meters. This land cover classification dataset employs images from Sentinel-1 and Sentinel-2 satellites to divide global land cover into 11 classes: built-up areas, barren/sparse vegetation, snow & ice, open water, trees, shrubland, grassland, cropland, herbaceous wetland, mangroves, moss and lichen. The ESA World Cover dataset has a high accuracy assessment rate of 74.4% (Tsendbazar, 2020). According to the ESA World Cover data, cropland is defined as “that part of the land which is covered with annual cropland and is sown/planted or harvested within a

³It is crucial for generating next-generation products such as land change detection maps, land cover maps, and various geophysical variables (Drusch et al., 2012). Sentinel-2A has a multi-spectral instrument (MSI) sensor, which measures radiation reflected from the Earth’s surface at multiple wavelengths. The range of wavelengths of electromagnetic radiation reflected by the Earth’s surface and detected by the satellite sensor constitutes a band. Sentinel-2 MSI, Level-1C captures radiation reflected from the Earth’s surface in thirteen bands.

⁴Landsat-8 is the eighth Landsat satellite in space and is a part of the U.S. Geological Survey (USGS) National Land Imaging (NLI) Program. It contains two sensors, the Operational Land Imager sensor (OLI) and the Thermal Infrared Sensor (TIS) (“Landsat Satellite Missions — U.S. Geological Survey”, n.d.).

year after the sowing or planting date” (Van De Kerchove, 2020). We mask every land cover class except cropland to prevent data contamination from other vegetation classes like grasslands, forests, and shrublands, which are irrelevant to our study (Figure A1 and Figure A2)

We employ an alternative land classification dataset, called the Copernicus Global Land Service: Land Cover dataset⁵ to verify our results from the ESA World Cover dataset. The notable advantage of utilizing this alternative dataset is its provision of land cover classification from 2015 to 2020, with a spatial resolution of 100 meters, which aligns with our study period (2015-2019). Consequently, this dataset enables us to accurately identify any instances of misidentified agricultural land in the ESA World Cover dataset. We use this data set to test the reliability and consistency of our findings. The absence of ground truthing (training data) prevents us from evaluating crop-wise productivity gains directly. Nonetheless, we address this limitation by verifying productivity gains specifically in cereal crops during the kharif and rabi seasons. To identify agricultural lands cultivated with cereal crops, we leverage the MODIS landcover type data provided by NASA USGS EROS Center.⁶ We identify agricultural land cultivated with cereals using the landcover classification type 1 (LC-Type5), corresponding to the Annual Plant Functional Types classification⁷. This classification allows us to ensure that we compare the productivity of similar crops, as we confirm the presence of common cereal crops in both the treatment and control regions from administrative data.

To check for the balance of covariates for the treatment and control region, which

⁵It defines agricultural areas as cultivated and managed land, specifically focused on agriculture. It includes annual crops sown and harvested in a year while excluding perennial crops. Therefore, the definition of agriculture in the Copernicus Global Land Service: Land Cover dataset aligns with the definition used in the ESA World Cover dataset.

⁶The MODIS Landcover type data utilizes supervised classification of machine learning techniques, offering five distinct types of classifications (Menashe and Friedl, 2018).

⁷Croplands are defined as areas primarily characterized by herbaceous vegetation less than 2 meters in height and with at least 60 per cent of the cultivated land dedicated to cereal crops.

might affect agricultural productivity, we use multiple datasets like Terra Climate SMAP etc, which contain agro-climatic information like rainfall, temperature, soil moisture etc. and are shown in Table A1

We chose to sample 100,000 cropland pixels, which are observed every month. The total population of ESA World Cover cropland pixels in our study region is 219,753,702.⁸ The chosen sample size of 100,000 pixels will ensure that a population proportion of 50% (the worst case) will be estimated at the 99% confidence level with a margin of error of only 0.41. See Table A3 for details.

4 Key Variables: Vegetation Indices

We use a remotely sensed index called the Normalised Difference Vegetation Index (NDVI) as the main variable to gauge agricultural productivity in treatment and control regions. The amount of vegetation on the ground correlates with the light reflected in the red and near-infrared (NIR) bands. The light reflected in the red band from croplands(vegetation) decreases as the crop moves from sowing to near the harvesting stage. This is due to the absorption of red light by chlorophyll present in photosynthetically active leaves. In contrast, the light reflected in the NIR band increases as plant development starts after sowing because of the scattering of light from healthy leaves (reflection, transmission)(A. Huete et al., 1999). Thus, NDVI can be used as a measure of production and productivity by calculating the amount of light reflected in the red and near-infrared band from croplands, which is captured by satellite sensors in space. NDVI is a ratio⁹ of reflectance of two bands, i.e., Red and near-infrared (ρ_{NIR}/ρ_{RED}), which is normalised and stan-

⁸(This is the largest total population of pixel among all the data we use. Therefore, in all other datasets used, we more than satisfy sample size requirement.

⁹NDVI as a ratio minimises noise associated with bands which arise due to variations in sun and view angles, topography, clouds and shadows due to clouds. Taking ratio is also important to control instrument and calibration-related errors(A. Huete et al., 1999)

standardised to have NDVI values between -1 to +1 (Deering, 1978; A. Huete et al., 1999). NDVI values close to zero represent bare soil; higher NDVI values mean more ground vegetation.

$$NDVI = \frac{[(\rho_{NIR}/\rho_{RED}) - 1]}{[(\rho_{NIR}/\rho_{RED}) + 1]} \quad (1)$$

Equation 1 can be also simply expressed as NIR to Red ratio

$$NDVI = \frac{[X_{NIR} - X_{RED}]}{[X_{NIR} + X_{RED}]} \quad (2)$$

ρ_{NIR} and ρ_{RED} represent the amount of light reflected in the near-infrared and red bands, respectively.

Additionally, we use the Enhanced Vegetation Index (EVI) to verify whether the results obtained from NDVI are robust to an alternative vegetation index. Using multisource data and multiple vegetation indices effectively enhances the accuracy and validity of remotely sensed phenology-related products (Wang et al., 2017). Compared to NDVI, EVI does not saturate over regions with high vegetation or biomass, and it is not affected by soil reflectance, cloud cover (A. Huete et al., 2002), and aerosol scattering (A. Huete et al., 1999).

$$EVI = \frac{\rho_{NIR} - \rho_{RED}}{\rho_{NIR} + C_1\rho_{RED} - C_2\rho_{BLUE} + L} * (1 + L) \quad (3)$$

EVI is a modified NDVI that incorporates a soil adjustment factor, L and C_1 , C_2 coefficients that use the blue band to correct the red band for atmospheric aerosol scattering. The values of L , C_1 and C_2 which has been empirically determined are 6, 7.5 and 1 respectively.

To account for the influence of soil brightness in areas with low vegetation cover

due to crops, we also use the soil-adjusted vegetation index (SAVI). SAVI helps compute vegetation indices in areas where crops grow in soils with different backgrounds. Although both the surface and subsurface soil moisture, which are important covariates, are well-balanced in both treatment and control regions (Table 1), the purpose of using SAVI is to eliminate any potential soil-induced variation that may arise due to other characteristics of the soil (A. R. Huete, 1988).

$$SAVI = \left(\frac{NIR - R}{NIR + R + L} \right) \cdot (1 + L) \quad (4)$$

where L is a soil brightness correction factor and is set to 0.5.

$$SAVI = \left(\frac{NIR - RED}{NIR + RED + L} \right) \cdot L \quad (5)$$

SAVI incorporates L as soil brightness correction factor (L) and $L = 0.5$

We also use the green chlorophyll vegetation index (GCVI) as an alternative index which helps estimate chlorophyll content in leaves of vegetation. The spectral reflectance of vegetation is related to chlorophyll content in the leaves (Gitelson et al., 2003). Thus GCVI also gives us an idea about the amount of green vegetation on the ground and, unlike NDVI, helps to overcome the problem of saturation over dense canopies. GCVI is calculated based on light reflected from vegetation and recorded by the sensor in NIR and green bands.

$$GCVI = \left(\frac{NIR}{Green} \right) - 1 \quad (6)$$

We also use the Normalised Difference Moisture Index (NDMI) to control for time-varying moisture levels in crop canopy to capture water stress conditions (Mashaba et al., 2016). NDMI is a ratio of light reflected in NIR and short wave infrared

band (SWIR)(“Normalized Difference Moisture Index — U.S. Geological Survey”, n.d.).

$$NDMI = \frac{NIR - SWIR}{NIR + SWIR} \quad (7)$$

5 Methodology

In this section, we discuss the research design and empirical specifications to be used for this study. We create a novel experimental design using the flexibility offered by satellite data. Instead of selecting the bordering districts as a whole, we select all areas in a radius of 10 km from the state border of Telangana on either side. This includes regions up to 10 km of the border in Telangana and regions up to 10 km inside neighbouring states.

5.1 Research Design

“Everything is related to everything else, but near things are more related than distant things” (Toblers First Law of Geography: Tobler, 1970)

The region 10 km within the Telangana border is the treatment area, and the region 10 km within the neighbouring state borders are the control regions. In Figure 1b, the regions in green are those up to 10 km inside Telangana and are regions where cash transfers were disbursed. The regions in grey are in neighbouring states and received no comparable transfers, and are control regions. Satellite images allow the flexibility to focus on areas of interest. By selecting treatment and control regions in this way, we minimize the differences between treatment and control regions along a variety of geographical and agro-climatic characteristics. A covariate balancing test between treatment and control regions demonstrates that

they do not differ in agro-climatic characteristics (Table 1). The only major difference that remains between these two regions is that they are exposed to different state policies. This simulates an experimental design that can be used to estimate causal effects due to a policy change.

As mentioned in the data section, we identify croplands in this border area with the help of the ESA World Cover dataset. After masking all land cover classes except cropland, we select a sample of 100,000 pixels by stratified random sampling from the 10 km border area of the agricultural land. Subsequently, we create a panel dataset covering 2017 to 2019, observing monthly NDVI, EVI, SAVI and GCVI values for each crop pixel. We then map the selected crop pixels to the district border region to determine which district they belong to. It gives us complete information about the crop pixels, such as sample size by bordering district and location of each pixel, allowing us to add pixel-location fixed effects and district-fixed effects. In Figure 1c, We show the distribution of crop pixels on the 10 km border region, with green polygons representing bordering districts of Telangana and blue polygons representing bordering districts of neighbouring states. The sample covers the 10 km border of Telangana, which is the treatment state, and the 10 km border of neighbouring states, including Andhra Pradesh, Maharashtra, Chhattisgarh, and Karnataka, which are the control states.

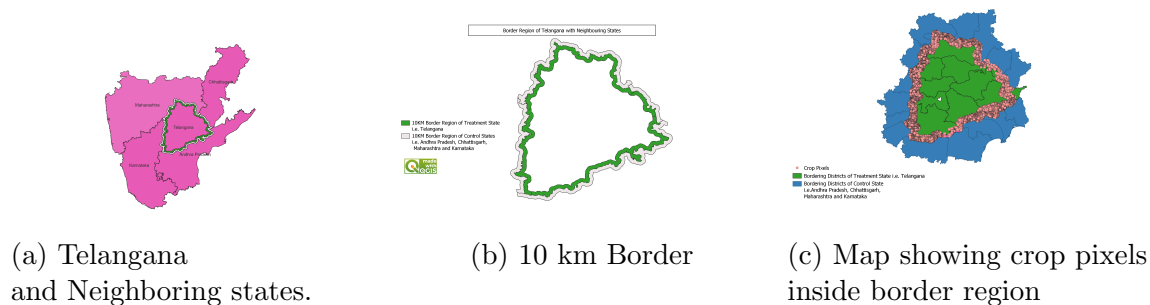


Figure 1: Border Design of the Study

Table 1: Covariate Balance Test

Variable	Unit	mean(Treatment,T)	mean(Control,C)	Difference(T-C)	t-value	p-value
Actual Evapo-Transpiration	mm	66.946	67.591	-0.644	-0.1	0.907
Potential Evapo-Transpiration	mm	136.887	137.094	-0.207	-0.05	0.962
Run off	mm	20.453	17.389	3.064	0.6	0.547
Minimum Temperature	°C	22.2	22.258	0.058	-0.1	0.904
Maximum Temperature	°C	33.402	33.469	-0.067	-0.15	0.887
Wind Speed	m/s	1.527	1.529	-0.002	0	0.984
Rainfall	mm	96.677	95.668	1.009	0.05	0.946
Surface Soil Moisture	mm	10.549	10.599	-0.051	-0.15	0.876
Sub Surface Soil Moisture	mm	76.931	79.382	-2.45	-1.05	0.301
Night Light Intensity	nanoWatts/cm2/sr	.437	.439	-0.002	-0.1	0.928

5.2 Empirical Specification

We use a simple difference-in-differences framework to estimate the impact of cash transfers on agricultural productivity. The following is the difference-in-differences specification:

$$VI_{itk} = \alpha_0 + \beta_1 \text{treat}_i + \beta_2 \text{post}_t + \beta_3 (\text{treat} \times \text{post})_{it} + \beta_4 \text{NDMI} + \gamma_p + \delta_d + \lambda_t + \epsilon_{itk} \quad (8)$$

VI_{it} in Equation 8 refers to a vegetation index (multiple indices are used) value at pixel ‘i’ in month ‘t’ in year ‘k’. Treat_i is a dummy variable with value 1 if pixel ‘i’ belongs to the treatment region, and 0 otherwise. Post_t is a dummy variable with value 1 if the observation is recorded after the treatment commences, and 0 otherwise (upto January 2014). There are three variants of Post_t : one includes all months in the year, one includes only the Kharif months (August-November), and another includes only the rabi months (January-April). $\text{Treat} \times \text{post}_{it}$ is the interaction term of interest (which also varies according to the definition of Post_t). β_3 yields the difference-in-differences coefficient. NDMI is a normalised difference moisture index that controls for time-varying moisture levels over space and time. γ_p represents pixel-fixed effects which will take care of a host of time-invariant pixel-

specific characteristics. δ_p represents district-fixed effects that control for time-invariant characteristics such as agronomic suitability, access to infrastructure etc. The term λ_t is for month-fixed effects (to account for annual seasonal variations). ϵ_{itk} is the random error term.

6 Dealing With Cloud Cover

In India, the kharif season from June to November is characterized by cloudy weather during the rainy days of the monsoon season. This can pose a challenge to estimating agricultural productivity using satellite data accurately when the light from the sun is in the form of electromagnetic radiation and encounters clouds and other materials in the atmosphere, a portion of it gets reflected. Consequently, the sensor used to measure this reflected light from the target (in this case, agricultural vegetation) records not only the reflected light from the target but also other light from the reflected radiation of the atmosphere. This additional light can lead to inaccurate estimates of agricultural productivity when using such data.

Therefore, it is essential to incorporate cloud masking techniques when using satellite data. We employ two methods to address the cloud cover problem. First, we apply a cloud mask to input images using the internal cloud masking algorithm of each dataset, setting mask values to zero for pixels corresponding to clouds or cirrus clouds¹⁰. Second, we create monthly composites of Sentinel-2, Landsat-8, and MODIS images to retain the best pixels of the month and fill temporal gaps caused by cloud masking restrictions (Lin et al., 2014; Sakamoto et al., 2005; Soriano-González et al., 2022; Tornos et al., 2015). By using these methods to deal with cloud cover, we obtain cloud-free satellite images that can reflect the best possible

¹⁰We use QA60 Bitmask bands of Sentinel-2 and the pixel_qa band of Landsat-8 data to remove pixels contaminated by clouds.

approximation of true productivity on the ground.

7 Results

From Figure 2, it can be seen that before the implementation of the cash transfer policy, there were no major differences in productivity trend between the treatment and control states during the kharif months (compare August to November before and after treatment). For the rabi months, the trends are less conclusive (we discuss this later on). Overall, the parallel trends indicate that the exposure of the treatment state (Telangana) to the cash transfer policy can be estimated using a difference-in-differences design.

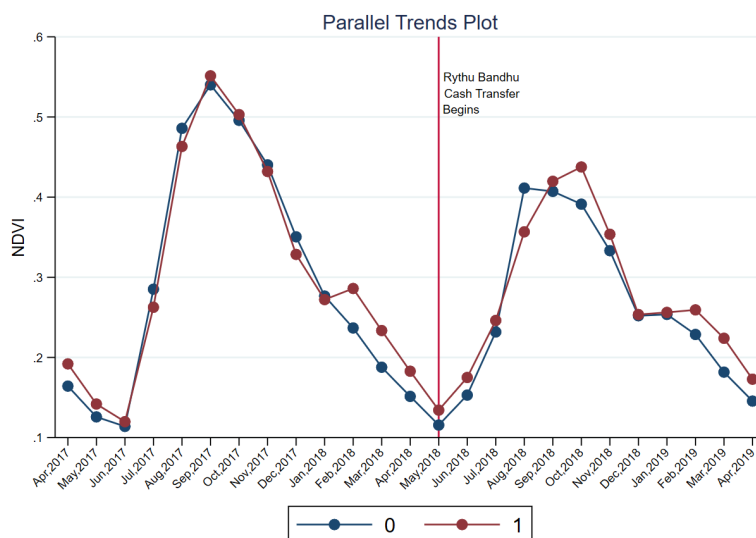


Figure 2: Parallel trends assumption is satisfied.

We present the main results in Table 2. These results are estimated according to the Equation 8 using data from Landsat 8 and the outcome variable here is NDVI.¹¹ Column (1) shows results from the base model without any controls, col-

¹¹The results are based on atmospherically corrected and cloud-processed surface reflectance data of Landsat 8. Landsat 8 uses the CFMASK algorithm for cloud processing and contains results in a quality assessment (QA) band in level 1 Landsat collection.

umn (2) shows results from the fully specified regression equation. The estimation is based on the full sample, covering all months of the year. To analyze cropping season-wise variations, we further investigate changes in NDVI for kharif and rabi crops (the two primary cropping seasons in India) in columns (3) and (4), respectively. We are interested in knowing the maximum NDVI values (full greenness) during the kharif season (which will correspond to actual crop stand in the ground), so we limit our sample to August, September, October, and November. The results in column (3) indicate a positive and statistically significant change in NDVI for kharif crops. The average NDVI of crop pixels within the treatment region is 0.017 standard deviations higher than those in the control region, indicating that the cash transfers changed crop productivity. For the rabi season, we restrict the sample to December to April and present the results in column (4). The findings suggest a smaller magnitude of effect compared to the kharif season, with the treatment region's NDVI being 0.015 standard deviations higher than the control region. To account for location-specific and time-invariant characteristics, we introduce pixel-fixed effects in our regression specification. These effects capture microclimate attributes at various crop pixel locations. Additionally, to control for time-invariant district-level characteristics, we include district-fixed effects. These include access to infrastructure such as roads, soil testing facilities, Krishi Vigyan Kendras (KVKS), and soil texture types. Moreover, we incorporate month-fixed effects to address seasonal variations and other unobservable time-specific characteristics. Our findings reveal a positive and significant impact of the cash transfer policy on NDVI for kharif and rabi crops, with kharif crops experiencing more pronounced productivity gains.

	(1)	(2)	(3)	(4)
VARIABLES	Base Model	Full Model	Kharif	Rabi
1.treat#1.post	0.012*** (0.000)	0.016*** (0.000)	0.017*** (0.001)	0.015*** (0.000)
treat = 1	0.022*** (0.000)			
post = 1	-0.027*** (0.000)	-0.051*** (0.000)	-0.096*** (0.000)	-0.055*** (0.000)
NDMI		-0.054*** (0.001)	-0.058*** (0.003)	0.119*** (0.003)
Observations	5,731,858	5,731,858	1,901,934	2,399,998
R-squared	0.001	0.410	0.322	0.472
Pixel Fixed Effects	No	Yes	Yes	Yes
District Fixed Effects	No	Yes	Yes	Yes
Month Fixed Effects	No	Yes	Yes	Yes
Robust SE	No	Yes	Yes	Yes

Standard errors in parentheses

*** p<0.01, ** p<0.05, * p<0.1

Table 2: Main results with NDVI (from Landsat 8) as outcome variable showing increases after cash transfer. Results are in standardised beta coefficients.

Table 3 presents results related to croplands where cereals are cultivated. We utilized the MODIS landcover classification dataset to identify areas where cereals are grown.¹² We randomly sample a population of 98,235 cereal pixels based on this

¹²This dataset is discussed in the data section of this paper.

dataset, representing our region’s cereal growing areas. The sample acts as a representative population of cereal pixels for this analysis. Although this approach does not allow us to estimate crop-specific productivity, it enables us to focus on a broad category of crops which includes rice, wheat, maize, and other cereals. The results presented in Table 3 confirm the productivity gains in cereals due to the cash transfer policy. Specifically, we compare different models, as shown in Table 2, to understand the impact of the policy. Column (1) shows results without any controls and includes full-year NDVI change estimates. Column (2) shows the full-year model with all controls. Column (3) and column (4) specifically focus on NDVI changes in kharif and rabi cereals, respectively. These columns use the same fixed effects as presented in Table 2. We observe a clear increase in NDVI for cereals in the treatment region (those who received the cash transfer policy) during both the kharif and rabi seasons. In column (3), NDVI for kharif cereals in the treatment region is 0.017 standard deviations higher than that of kharif cereals in the control region. Our findings for rabi cereals are consistent with the results in Table 2, where the magnitude of change in NDVI is smaller than kharif cereals. In column (4), we find that the treatment regions, which received the cash transfer policy, experienced a 0.012 standard deviations increase in NDVI for rabi cereals compared to the control regions. Our analysis indicates a positive effect of the cash transfer policy on cereal productivity, evident from the increase in NDVI values in the treatment regions compared to the control regions for both kharif and rabi cereals.

	(1)	(2)	(3)	(4)
VARIABLES	Base Model	Full Model	Kharif	Rabi
1.treat#1.post	0.008*** (0.000)	0.011*** (0.000)	0.017*** (0.000)	0.012*** (0.000)
treat = 1	0.016*** (0.000)			
post = 1	-0.027*** (0.000)	-0.050*** (0.000)	-0.098*** (0.000)	-0.060*** (0.000)
NDMI		-0.015*** (0.000)	-0.046*** (0.000)	0.163*** (0.000)
Observations	6,032,595	6,032,595	1,875,780	2,360,230
R-squared	0.001	0.418	0.306	0.502
Pixel Fixed Effects	No	Yes	Yes	Yes
District Fixed Effects	No	Yes	Yes	Yes
Month Fixed Effects	No	Yes	Yes	Yes
Robust SE	No	Yes	Yes	Yes

Standard errors in parentheses

*** p<0.01, ** p<0.05, * p<0.1

Table 3: Cereals-only results with NDVI (from Modis 500 Landcover) as outcome variable showing increases after cash transfer. Results are in standardised beta coefficients.

8 Robustness

In this section, we discuss the results of various robustness checks we carry out to verify our main results. These checks include placebo regressions for the last two years of each kharif and rabi season. We re-estimate our main results with alternative datasets (with different spatial resolutions), other vegetation indices, and another cropland classifying dataset from the Copernicus Global Land Cover (Collection 3).

8.1 Placebos confirm results

Placebo regressions involve employing the same sample and regression model but with a “fake” treatment for years in which we expect no causal impact, i.e. the productivity of the treatment region is expected to be lower or equal to that of the control region. We run our main regressions using cut-offs in the past two years to check if productivity was rising on the Telangana side before the cash transfers. We run these separately for the kharif and rabi seasons.

	(1)	(2)	(3)	(4)
VARIABLES	Kharif:t-1	Kharif:t-2	Rabi: t-1	Rabi: t-2
1.treat#1.post	-0.013*** (0.001)	-0.036*** (0.001)	0.018*** (0.000)	0.001 (0.000)
NDMI	-0.028*** (0.003)	-0.022*** (0.004)	0.125*** (0.004)	0.128*** (0.004)
Observations	1,529,397	1,164,205	1,999,998	1,599,998
R-squared	0.312	0.350	0.469	0.473
Pixel Fixed Effects	Yes	Yes	Yes	Yes
District Fixed Effects	Yes	Yes	Yes	Yes
Month Fixed Effects	Yes	Yes	Yes	Yes
Robust SE	Yes	Yes	Yes	Yes

Robust standard errors in parentheses

*** p<0.01, ** p<0.05, * p<0.1

Table 4: Placebo regression of two past years

Ideally, the placebos should show that productivity either did not change or has an opposite sign from the main result. The first two columns of Table 4 suggest that the productivity of the treatment region is indeed lower than that of the control region in the kharif season. In the case of rabi seasons the placebos are less clear. The year before the treatment, rabi productivity saw an improvement on the Telangana side compared to the control regions. While two years prior to the cash transfers, rabi productivity change was not different in the treatment and control

regions.

A notable pattern emerges for kharif, the main cropping season. Productivity change was positive and significant in Telangana only when the cash transfer was provided, while in two previous years, Telangana was worse off than the control states. We can be confident that the cash transfer policy led to increased agricultural productivity for kharif crops. The rabi pattern is less conclusive.

8.2 Alternative data shows similar results

	(1)	(2)	(3)	(4)
VARIABLES	S2_Kharif	Modis_Kharif	S2_Rabi	Modis_Rabi
1.treat#1.post	0.039*** (0.001)	0.019*** (0.000)	0.013*** (0.000)	0.015*** (0.000)
post = 1	-0.237*** (0.001)	-0.088*** (0.000)	-0.043*** (0.000)	-0.022*** (0.000)
NDMI	0.171*** (0.005)	0.235*** (0.002)	0.236*** (0.003)	0.402*** (0.003)
Observations	599,625	1,994,840	1,187,668	2,399,400
R-squared	0.516	0.490	0.591	0.690
Pixel Fixed Effects	Yes	Yes	Yes	Yes
District Fixed Effects	Yes	Yes	Yes	Yes
Month Fixed Effects	Yes	Yes	Yes	Yes
Robust SE	Yes	Yes	Yes	Yes

Robust standard errors in parentheses

*** p<0.01, ** p<0.05, * p<0.1

Table 5: Results in alternative datasets with NDVI as the outcome variable.

Table 5 presents results from other satellites, namely Sentinel-2 and MODIS-250, to assess the robustness of our NDVI estimates. By using NDVI data from these satellites with different spatial resolutions, we aim to check the consistency of our the main results from Landsat-8. Sentinel-2 offers high-resolution data with a spatial resolution of 10 meters, providing a more granular view of croplands. We utilize the multispectral instrument data from Sentinel-2 and the QA60 band for cloud masking (Delwart, n.d.). To ensure data quality, we apply strict restrictions, retaining only images with a cloud cover of 20% or less for vegetation index calculations. This approach helps us minimize errors associated with cloud interference. In column (1) and column (3) of Table 5, we report the results of kharif NDVI and rabi NDVI, respectively, based on Sentinel-2 data. Our analysis shows a significant increase of 0.039 standard deviations in kharif NDVI for the treatment region compared to the control region. Similarly, for the rabi season, the treatment regions exhibit 0.013 standard deviations higher NDVI than the control regions. Notice that sign of these results is the same as the main results.

We then estimate NDVI change using MODIS-250 data (with a coarse resolution of 250 m). Columns (2) and (4) present the results of MODIS-250-based NDVI for the kharif and rabi seasons, respectively. In the kharif season, the treatment regions experienced a notable increase of 0.019 standard deviations in NDVI compared to the control region. Similarly, in the rabi season, the treatment regions observed a 0.015 standard deviations increase in NDVI. Here again, the sign of the coefficients has remained consistent.

The results from alternative datasets consistently show a smaller magnitude of NDVI change during the rabi season compared to the kharif season. This observation aligns with the outcomes from Table 2 and Table 3.

8.3 Alternative indicators align with NDVI

	(1)	(2)	(3)	(4)	(5)	(6)
VARIABLES	EVI_Kharif	GCVI_Kharif	SAVI_Kharif	EVI_Rabi	GCVI_Rabi	SAVI_Rabi
1.treat#1.post	0.001 (0.197)	0.008*** (0.005)	0.017*** (0.001)	0.000 (0.049)	0.003*** (0.005)	0.015*** (0.001)
post = 1	-0.002* (0.152)	-0.047*** (0.003)	-0.096*** (0.001)	-0.002** (0.035)	-0.026*** (0.002)	-0.055*** (0.000)
NDMI	-0.003*** (0.588)	-0.005*** (0.019)	-0.058*** (0.004)	0.009*** (0.222)	0.047*** (0.020)	0.119*** (0.005)
Observations	1,902,091	1,902,091	1,902,091	2,400,000	2,400,000	2,400,000
R-squared	0.053	0.157	0.322	0.042	0.128	0.472
Pixel Fixed Effects	Yes	Yes	Yes	Yes	Yes	Yes
District Fixed Effects	Yes	Yes	Yes	Yes	Yes	Yes
Month Fixed Effects	Yes	Yes	Yes	Yes	Yes	Yes
Robust SE	Yes	Yes	Yes	Yes	Yes	Yes

Robust standard errors in parentheses

*** p<0.01, ** p<0.05, * p<0.1

Table 6: Results in alternative indicators from Landsat.

Table 6 presents the results another robustness check, where we evaluate productivity change using alternative vegetation indices, namely EVI (Enhanced Vegetation Index), GCVI (Green Chlorophyll Vegetation Index), and SAVI (Soil-Adjusted Vegetation Index). These indices offer advantages over NDVI, as previously discussed in the key variables section, by accounting for various factors such as dense crop stands, cloud cover, soil reflectance, atmospheric and aerosol scattering, and other soil-induced variations. The objective of this analysis is to corroborate the findings from the main results section and examine whether the results hold consistently when measuring productivity changes through EVI, GCVI, and SAVI.

In Table 6, we report the estimates of Landsat-8 based alternative vegetation indices for both the kharif and rabi seasons. Notably, all vegetation indices exhibit positive and statistically significant beta (standardized) coefficients, except EVI. Nevertheless, both the Sentinel-2 and MODIS-250 based EVI estimates in Table A8 and Table A9, respectively, are positive and significant.

We also present alternative indicator results from Sentinel 2 (Table A8) and MODIS-250 (Table A9). Here too we see that the signs of productivity change are consistent ¹³. Magnitudes of change too vary in a tight band.

An important observation from these results is that the magnitude of GCVI, and SAVI estimates for the rabi season consistently appear smaller than those for the kharif season. This pattern aligns with the findings from Table 2, Table 3, and Table 5, further reinforces our results. It provides additional evidence supporting the notion that the cash transfer policy has indeed increased the productivity of the treatment region.

¹³GCVI in kharif from Sentinel 2 is an exception

8.4 Alternative land classification show same results

	(1)	(2)	(3)	(4)
VARIABLES	Base Model	Full Model	Kharif	Rabi
1.treat#1.post	0.011*** (0.000)	0.015*** (0.000)	0.016*** (0.000)	0.016*** (0.000)
treat = 1	0.025*** (0.000)			
post = 1	-0.027*** (0.000)	-0.053*** (0.000)	-0.096*** (0.000)	-0.055*** (0.000)
NDMI		-0.043*** (0.000)	-0.061*** (0.000)	0.112*** (0.000)
Observations	6,130,778	6,130,778	1,901,067	2,399,997
R-squared	0.001	0.407	0.322	0.473
Pixel Fixed Effects	No	Yes	Yes	Yes
District Fixed Effects	No	Yes	Yes	Yes
Month Fixed Effects	No	Yes	Yes	Yes
Robust SE	No	Yes	Yes	Yes

Standard errors in parentheses

*** p<0.01, ** p<0.05, * p<0.1

Table 7: Results in alternative land classification from Landsat.

In Table 7, we present the results of an additional robustness check, where we estimate NDVI derived from Landsat-8 satellite, using light reflected in red and infrared wavelengths at various cropland locations identified through the Copernicus landcover classification (Collection 3) dataset. This dataset, discussed in the

data section, provides information about various landcover classes with a spatial resolution of 100m for 2015-2020. The purpose of this robustness check is to investigate whether our results remain consistent when we identify croplands based on the Copernicus landcover dataset, as opposed to using the ESA WorldCover dataset. Although the latter offers a higher resolution (10m), it is only available from 2020 onwards. For our analysis, we limit the data to 2019, as we aim to avoid any potential data anomalies due to the COVID-19 pandemic that began in March 2020. We assumed that croplands would not change significantly over short intervals of time. We evaluate if there is a significant mismatch between the croplands identified through ESA WorldCover 2020 and the actual croplands in our study period (2018-2019). Any substantial mismatch could potentially affect the stability of our results when we change the sample of crop pixels to the Copernicus landcover dataset.

The sample used for NDVI estimation in Table 7 differs in two ways. First, we identify croplands based on a different data source than ESA, which was used for the main results. Second, we re-randomize the sample, this time with a different seed number, resulting in crop pixels being randomly distributed to form a sample from different locations than those used in the ESA WorldCover-based sample. In Column (3) of Table 7, we find that the treatment region exhibits NDVI values 0.016 standard deviations higher than the control region for kharif crops and 0.016 standard deviations higher for rabi crops.

The replication of our main results from Table 2 in Table 7 demonstrates that our findings are robust to changes in the sample. This indicates that the observed impact of the cash transfer policy on productivity is not a random occurrence that is driven by the sample that we happen to sample.

8.5 Results hold with varied clustering

Finally, in Table A10 we present the main results at two different levels of clustering of standard errors. Our main results are robust standard errors that are clustered at pixel-level. This is not always convincing. Since our design is non-standard and the obvious clustering units which are districts and states are too few, we resort to alternative approaches to evaluate our errors. We follow state-location and district-location clustering. We generate a variable at the degree-minute level using geographic coordinates and interact them with state and district units, respectively. Our main results are clustered too granularly, which may lead to under-estimated errors. The district-location clusters are more coarse, while state-location clusters are even more coarse. We find that the results hold across these two variations. Our results are not sensitive to the level of error clustering.

9 Discussion and Conclusions

Lack of pre-implementation data constrains the evaluation of many policies. In this study, we aim to evaluate an agricultural policy designed to enhance agricultural productivity, despite such data limitations. We leverage high-resolution satellite data and a custom border design to assess the impact of a cash transfer policy implemented in Telangana, a southern state in India.

Rather than relying on entire district borders, we precisely carve treatment and control areas within a 10 km radius from the shared border. This approach minimises covariate imbalances and provides us with precise productivity estimates. Due to the lack of administrative/survey data at a granular level, we exclusively depended on remote sensing data from various satellites, each offering distinct spatial and temporal resolutions, as well as internal cloud processing algorithms.

Our findings demonstrate that the cash transfer policy has increased productivity in the state. The season-wise analysis indicates a clearer effect of the policy on the productivity of kharif crops (the main cropping season), while its impact on rabi crops is less clear. Although our data limitations prevent a detailed analysis of productivity for individual crops in the region, we have addressed this by focusing on the vital category of cereal crops, which reinforces our conclusions. Placebo regressions confirm our claim, supporting the increase in agricultural productivity due to the cash transfer policy, primarily for kharif crops.

Specifically, our estimates show a 0.017 standard deviation increase in NDVI for treatment regions compared to control regions during the kharif season and a 0.015 standard deviation increase during the rabi season. Regarding cereal crops, our results reveal a 0.017 standard deviation increase in NDVI for Kharif and a 0.012 standard deviation increase during the rabi season due to the cash transfer policy.

We ensure that the results are robust by testing them with various satellite data, alternative productivity indicators, and different samples. However, the absence of ground truthing data or training data limited our ability to verify results on a crop-wise basis.

The sign of productivity change is consistently positive across all specifications (Table 2), samples (Table 3) datasets (Table 5), and indicators (Table 6, Table A8, Table A9).¹⁴ To appreciate these results, compare them with placebo results in Table 4, where negative changes in productivity occur during the kharif season the previous two years.

The results vary within a tight range and are consistent in terms of the magnitude of productivity change. The kharif productivity change according to NDVI, for in-

¹⁴The only estimate that is negative and insignificant is for GCVI from Sentinel 2 for kharif in column (2) in Table A8, with a value of 0

stance, is between 0.016 standard deviations in the Copernicus classified Landsat 8 data to 0.039 standard deviations in Sentinel 2 (compare Table 2, Table 3, Table 5, and Table 7). Similarly, rabi productivity change in terms of NDVI has also varied in a tight range of 0.012-0.016 standard deviations (compare Table 2, Table 5, and Table 7).

In terms of the percentage change of yields (quantity of output per unit area cultivated), we provide an approximate equivalence relative to NDVI change. We estimate the main results using the logarithm of NDVI to estimate coefficients in percentage change terms in Table A11. Separately we use long-term administrative yield data at the district level and correlate those with NDVI over the same period (similar to Asher and Novosad, 2020) in Table A16. The estimated impact of cash transfers on the increase in productivity during the kharif season would be approximately 2.69 percent for Sentinel-2, 1.98 percent for Landsat-8, and 1.47 percent for Modis-250 based estimates¹⁵. The overall productivity increase attributed to cash transfers in the kharif season ranges from 1.47 per cent to 2.69 per cent. For the rabi season, the observed yield changes due to cash transfers amount to around 0.61 percent for Sentinel-2, 0.90 percent for Landsat-8, and 0.76 percent for Modis-250 based estimates¹⁶. The overall productivity increase attributed to cash transfers in the rabi season ranges from 0.61 percent to 0.76 percent.

Our study demonstrates the enormous potential of high-resolution satellite data, enabling researchers and policymakers to evaluate various policies that otherwise remain unexplored due to the lack of ground survey data. The custom border design we develop is adaptable and can be tailored to suit the requirements of policy evaluations of various kinds. Moreover, our approach to evaluating the cash trans-

¹⁵Derived from calculations using specific coefficients: $1.082*2.486$, $0.795*2.486$, and $0.592*2.486$

¹⁶Derived from calculations using specific coefficients: $0.419*1.458$, $0.620*1.458$, and $0.519*1.458$, respectively

fer policy using satellite data and the new border design is generalizable and can be applied worldwide to evaluate various policy interventions beyond agriculture. Our approach is only constrained by what satellite imagery can reliably measure.

References

- Abman, R., & Carney, C. (2020). Agricultural productivity and deforestation: Evidence from input subsidies and ethnic favoritism in Malawi. *Journal of Environmental Economics and Management*, *103*, 102342. <https://doi.org/10.1016/j.jeem.2020.102342>
- Agarwala, M., Bhattacharjee, S., & Dasgupta, A. (2022). Unintended consequences of Indian groundwater preservation law on crop residue burning. *Economics Letters*, *214*, 110446. <https://doi.org/10.1016/j.econlet.2022.110446>
- Ambler, K., De Brauw, A., & Godlonton, S. (2020). Cash transfers and management advice for agriculture: Evidence from senegal. *The World Bank Economic Review*, *34*(3), 597–617.
- Ambler, K., de Brauw, A., & Godlonton, S. (2020). Cash Transfers and Management Advice for Agriculture: Evidence from Senegal [Publisher: Oxford University Press]. *World Bank Economic Review*, *34*(3), 597–617. <https://doi.org/10.1093/wber/lhz005>
- Asher, S., & Novosad, P. (2020). Rural Roads and Local Economic Development. *American Economic Review*, *110*(3), 797–823. <https://doi.org/10.1257/aer.20180268>
- Blakeslee, D., Dar, A., Fishman, R., Malik, S., Pellegrina, H. S., & Bagavathinathan, K. S. (2023). Irrigation and the spatial pattern of local economic development in India. *Journal of Development Economics*, *161*, 102997. <https://doi.org/10.1016/j.jdeveco.2022.102997>

- Boone, R., Covarrubias, K., Davis, B., & Winters, P. (2013). Cash transfer programs and agricultural production: The case of malawi. *Agricultural Economics*, *44*(3), 365–378.
- Deering, D. W. (1978). *Rangeland reflectance characteristics measured by aircraft and spacecraftsensors*. Texas A&M University.
- Deining, K., Ali, D. A., Kussul, N., Shelestov, A., Lemoine, G., & Yailimova, H. (2023). Quantifying war-induced crop losses in Ukraine in near real time to strengthen local and global food security. *Food Policy*, *115*, 102418. <https://doi.org/10.1016/j.foodpol.2023.102418>
- Delwart, S. (n.d.). ESA standard document. (1).
- Drusch, M., Del Bello, U., Carlier, S., Colin, O., Fernandez, V., Gascon, F., Hoersch, B., Isola, C., Laberinti, P., Martimort, P., et al. (2012). Sentinel-2: Esa’s optical high-resolution mission for gmes operational services. *Remote sensing of Environment*, *120*, 25–36.
- Evans, D. K., Holtmeyer, B., & Kosec, K. (2019). Cash transfers and health: Evidence from tanzania. *The World Bank Economic Review*, *33*(2), 394–412.
- Gazeaud, J., & Stephane, V. (2023). Productive Workfare? Evidence from Ethiopia’s Productive Safety Net Program [eprint: <https://onlinelibrary.wiley.com/doi/pdf/10.1111/ajae.12310>]. *American Journal of Agricultural Economics*, *105*(1), 265–290. <https://doi.org/10.1111/ajae.12310>
- Gertler, P. J., Martinez, S. W., & Rubio-Codina, M. (2012). Investing cash transfers to raise long-term living standards. *American Economic Journal: Applied Economics*, *4*(1), 164–192.
- Gitelson, A. A., Gritz, Y., & Merzlyak, M. N. (2003). Relationships between leaf chlorophyll content and spectral reflectance and algorithms for non-destructive chlorophyll assessment in higher plant leaves. *Journal of plant physiology*, *160*(3), 271–282.

- Huete, A., Didan, K., Miura, T., Rodriguez, E. P., Gao, X., & Ferreira, L. G. (2002). Overview of the radiometric and biophysical performance of the modis vegetation indices. *Remote sensing of environment*, *83*(1-2), 195–213.
- Huete, A., Justice, C., & Van Leeuwen, W. (1999). Modis vegetation index (mod13). *Algorithm theoretical basis document*, *3*(213), 295–309.
- Huete, A. R. (1988). A soil-adjusted vegetation index (savi). *Remote sensing of environment*, *25*(3), 295–309.
- Jaafar, H. H., & Woertz, E. (2016). Agriculture as a funding source of ISIS: A GIS and remote sensing analysis. *Food Policy*, *64*, 14–25. <https://doi.org/10.1016/j.foodpol.2016.09.002>
- Landsat satellite missions — u.s. geological survey.* (n.d.). Retrieved March 22, 2023, from <https://www.usgs.gov/landsat-missions/landsat-satellite-missions>
- Lin, W., Zhang, F.-c., Jing, Y.-s., Jiang, X.-d., Yang, S.-b., & HAN, X.-m. (2014). Multi-temporal detection of rice phenological stages using canopy spectrum. *Rice Science*, *21*(2), 108–115.
- Mashaba, Z., Chirima, G., Botai, J., Combrinck, L., & Munghemzulu, C. (2016). Evaluating spectral indices for winter wheat health status monitoring in bloemfontein using lsat 8 data. *South African Journal of Geomatics*, *5*(2), 227–243.
- Menashe and Friedl. (2018, May 14). User guide to collection 6 MODIS land cover (MCD12q1 and MCD12c1) product. https://lpdaac.usgs.gov/documents/101/MCD12_User_Guide_V6.pdf
- Minhaz, A. (2023, March 9). *Rythu bandhu: A lifeline scheme for farmers in telangana* [Section: Agriculture]. Retrieved April 19, 2023, from <https://frontline.thehindu.com/the-nation/agriculture/rythu-bandhu-scheme-in-telangana-a-success-but-more-needs-to-be-done/article66571551.ece>
- Muralidharan, K., Niehaus, P., Sukhtankar, S., & Weaver, J. (2021). Improving Last-Mile Service Delivery Using Phone-Based Monitoring. *American Eco-*

- Journal of Applied Economics*, 13(2), 52–82. <https://doi.org/10.1257/app.20190783>
- Normalized difference moisture index — u.s. geological survey.* (n.d.). Retrieved July 24, 2023, from <https://www.usgs.gov/landsat-missions/normalized-difference-moisture-index>
- OECD. (2022). *Agricultural Policy Monitoring and Evaluation 2022*. <https://doi.org/https://doi.org/https://doi.org/10.1787/7f4542bf-en>
- Prifti, E., Daidone, S., & Davis, B. (2019). Causal pathways of the productive impacts of cash transfers: Experimental evidence from lesotho. *World Development*, 115, 258–268.
- Ramesh, P. (2020). *Cash transfers as a policy instrument in agriculture: Study of the rythu bandhu scheme and the land record updation programme in telangana* (Doctoral dissertation). Tata Institute of Social Sciences Mumbai.
- Sakamoto, T., Yokozawa, M., Toritani, H., Shibayama, M., Ishitsuka, N., & Ohno, H. (2005). A crop phenology detection method using time-series modis data. *Remote sensing of environment*, 96(3-4), 366–374.
- Shaw, A., Rathi, S., & Chakrabati, A. S. (2023). Cash Transfers and Landholding Inequality. Retrieved July 28, 2023, from <https://papers.ssrn.com/abstract=4523110>
- Soriano-González, J., Angelats, E., Martínez-Eixarchb, M., & Alcaraz, C. (2022). Monitoring rice crop and yield estimation with sentinel-2 data. *Field Crops Research*, 281, 108507.
- Thomas, S., Uday, D., & Zaveri, B. (2020). *Linking welfare distribution to land records: A case-study of the Rythu Bandhu Scheme (RBS) in Telangana* (tech. rep. TR-2020-4-27). Indira Gandhi Institute for Development Research. https://ifrogs.org/PDF/rbs_report.pdf

- Tobler, W. R. (1970). A computer movie simulating urban growth in the detroit region. *Economic geography*, 46(sup1), 234–240.
- Todd, J. E., Winters, P. C., & Hertz, T. (2010). Conditional cash transfers and agricultural production: Lessons from the oportunidades experience in mexico. *The Journal of Development Studies*, 46(1), 39–67.
- Tornos, L., Huesca, M., Dominguez, J. A., Moyano, M. C., Cicuendez, V., Recuero, L., & Palacios-Orueta, A. (2015). Assessment of modis spectral indices for determining rice paddy agricultural practices and hydroperiod. *ISPRS Journal of Photogrammetry and Remote Sensing*, 101, 110–124.
- Tsendbazar, N. (Ed.). (2020). World Cover Product Validation Report.
- Van De Kerchove, R. (Ed.). (2020). World Cover Product User Manual V1.0.
- Wang, C., Li, J., Liu, Q., Zhong, B., Wu, S., & Xia, C. (2017). Analysis of differences in phenology extracted from the enhanced vegetation index and the leaf area index. *Sensors*, 17(9), 1982.

1.1 Dataset Details

Table A1: Details of the Data sets to be used

Source	Spatial Resolution	Frequency	Variables used
Harmonised Sentinel-2 MSI: Multispectral Instrument, level -1C	10m	10 days	Vegetation Indices
LANDSAT/LC08/C01/T1_SR	30m	8 days	Vegetation Indices
MODIS-250 Terra	250m	16 days	Vegetation Indices
ESA WorldCover	10m	Annual	Croplands
CHIRPS Daily	5566m	Daily	Rainfall Data
Terraclimate	4638.3m	Monthly	Temperature
Terraclimate	4638.3m	Monthly	AET
Terraclimate	4638.3m	Monthly	PET
Terraclimate	4638.3m	Monthly	Runoff
Terraclimate	4638.3m	Monthly	Temperature
Terraclimate	4638.3m	Monthly	Wind Speed
VIIRS & Night Composites	463.83m	Monthly	Night Lights
Copernicus Landcover	100m	Annual	Croplands
MODIS-500 Land Cover Type	500m	Annual	Cereal Crops
NASA-USDA Enhanced SMAP	10000m	Monthly	Surface Soil Moisture Data
NASA-USDA Enhanced SMAP	10000m	Monthly	Subsurface Soil Moisture Data

1.2 Visual examples of masking

1.3 Sample size calculations

Table A2: Pixel Count by various landcover classes in ESA World Cover.

Landcover Class	Number of Pixels
Tree cover	94918096
Shrubland	31137867
Grassland	27787072
Cropland	219753702
Built-up	4580369
Bare/sparse vegetation	13478684
Snow and ice	0
Permanent water bodies	12424531
Herbaceous wetland	196941
Mangroves	0
Moss and lichen	0
Total Population of Pixels	404277262

Table A3: Sample Size Calculation for Sample of ESA WorldCover Crop Pixels.

Confidence Level (%)	Margin of Error (%)	Population Size	Population Proportion (%)	Required Sample Size
99	2.5	404277262	54.36	2643
99	2	404277262	54.36	4129
99	1.5	404277262	54.36	7340
99	1	404277262	54.36	16514
99	0.5	404277262	54.36	66048
95	2.5	404277262	54.36	1525
95	2	404277262	54.36	2383
95	1.5	404277262	54.36	4236
95	1	404277262	54.36	9531
95	0.5	404277262	54.36	38121

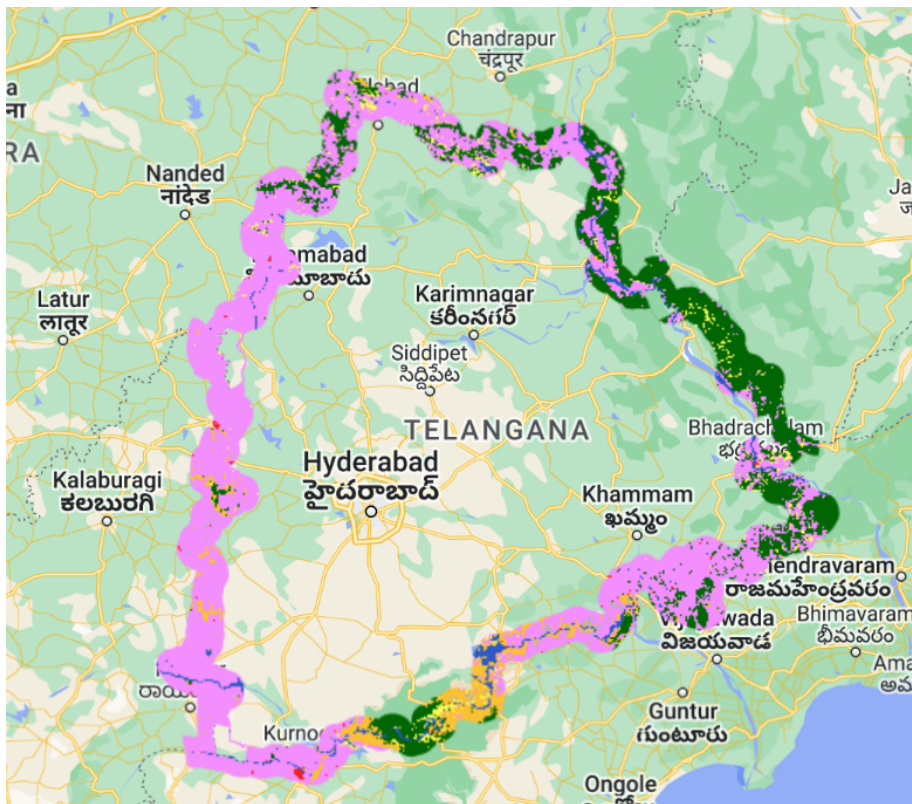


Figure A1: Unmasked image displaying the various landcover classes across the study area according to ESA WorldCover dataset

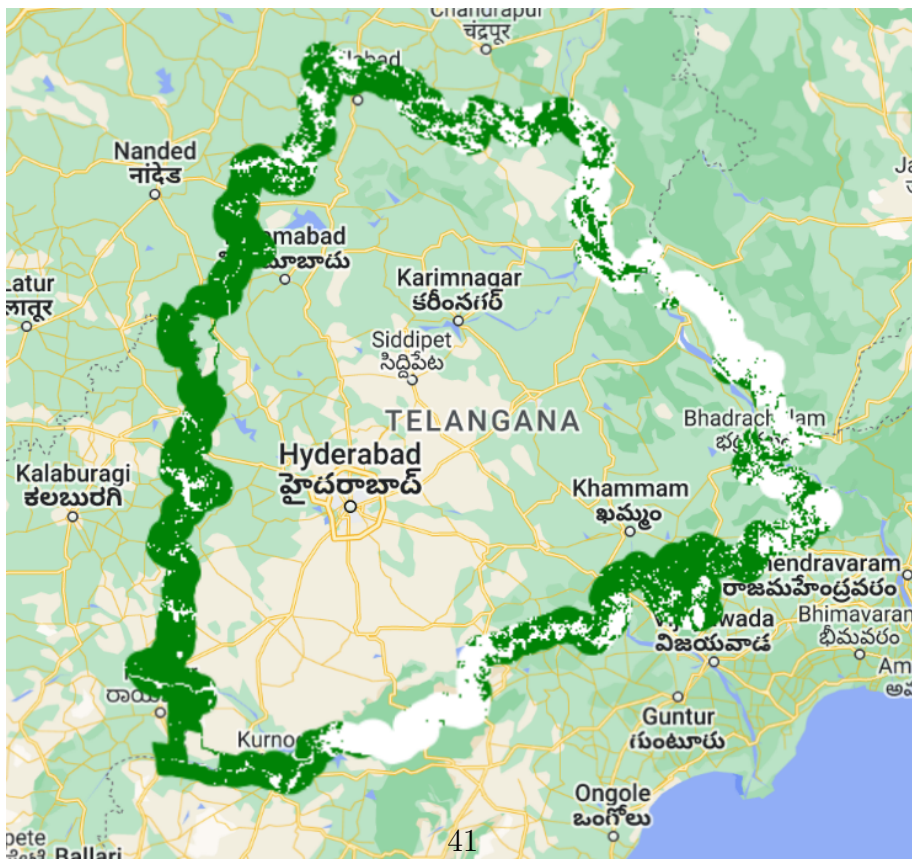


Figure A2: Masked image of ESA WorldCover dataset, where white areas indicate masked regions encompassing all landcover classes except cropland, while green areas represent croplands.

Table A4: Sample size required to accurately estimate a population proportion of 50% (the worst case) from a population of 219,753,702 pixels from ESA World-Cover Cropland classification

Confidence Level (%)	Margin of Error (%)	Minimum Sample Size Required
99	1	16,640
99	0.5	66,544
95	1	9,604
95	0.5	38,410

Table A6: Sample Size Calculation for Sample of ESA Copernicus Global Land-Cover Crop Pixels.

Confidence Level (%)	ME (%)	Population Proportion (%)	Population Size	Sample Size Required
99	2.5	64.35	4247633	2444
99	2	64.35	4247633	3818
99	1.5	64.35	4247633	6787
99	1	64.35	4247633	15271
99	0.5	64.35	4247633	61082
95	2.5	64.35	4247633	1411
95	2	64.35	4247633	2204
95	1.5	64.35	4247633	3917
95	1	64.35	4247633	8813
95	0.5	64.35	4247633	35252

Table A7: Pixel Count by various landcover classes in MODIS LandCover

Landcover Class	Number of Pixels
Water Bodies (0)	968
Evergreen Needleleaf Trees (1)	4
Evergreen Broadleaf Trees (2)	529
Deciduous Needleleaf Trees (3)	0
Deciduous Broadleaf Trees (4)	30230
Shrub (5)	125
Grass (6)	19412
Cereal Croplands (7)	98343
Broadleaf Croplands (8)	2549
Urban and Built-up Lands (9)	1333
Permanent Snow and Ice (10)	0
Non-Vegetated Lands (11)	311
Total Population of Pixels	153804

1.4 Alternative Indicators from Sentinel 2 and Modis 250

VARIABLES	(1)	(2)	(3)	(4)	(5)	(6)
	EVI_Kharif	GCVI_Kharif	SAVI_Kharif	EVI_Rabi	GCVI_Rabi	SAVI_Rabi
1.treat#1.post	0.021*** (0.001)	-0.000 (0.028)	0.016*** (0.000)	0.010*** (0.000)	0.007*** (0.001)	0.013*** (0.000)
post = 1	-0.194*** (0.001)	-0.042*** (0.019)	-0.225*** (0.000)	-0.033*** (0.000)	-0.072*** (0.001)	-0.059*** (0.000)
NDMI	0.117*** (0.007)	0.020*** (0.066)	0.144*** (0.000)	0.232*** (0.003)	0.236*** (0.011)	0.227*** (0.000)
Observations	599,609	599,627	599,625	1,187,664	1,187,671	1,187,668
R-squared	0.383	0.162	0.466	0.563	0.464	0.555
Pixel Fixed Effects	Yes	Yes	Yes	Yes	Yes	Yes
District Fixed Effects	Yes	Yes	Yes	Yes	Yes	Yes
Month Fixed Effects	Yes	Yes	Yes	Yes	Yes	Yes
Robust SE	Yes	Yes	Yes	Yes	Yes	Yes

Robust standard errors in parentheses

*** p<0.01, ** p<0.05, * p<0.1

Table A8: Results in alternative indicators from Sentinel 2.

	(1)	(2)
VARIABLES	EVI_Kharif	EVI_Rabi
1.treat#1.post	0.002*** (0.000)	0.011*** (0.000)
post = 1	-0.105*** (0.000)	-0.030*** (0.000)
NDMI	0.236*** (0.001)	0.365*** (0.002)
Observations	1,995,383	2,399,715
R-squared	0.445	0.647
Pixel Fixed Effects	Yes	Yes
District Fixed Effects	Yes	Yes
Month Fixed Effects	Yes	Yes
Robust SE	Yes	Yes

Robust standard errors in parentheses

*** p<0.01, ** p<0.05, * p<0.1

Table A9: Results in alternative indicators from Modis 250.

1.5 Results with Clustered Standard Errors

	(1)	(2)	(3)	(4)
VARIABLES	Kharif	Kharif	Rabi	Rabi
1.treat#1.post	0.017*** (0.002)	0.017*** (0.002)	0.015*** (0.001)	0.015*** (0.001)
post = 1	-0.096*** (0.001)	-0.096*** (0.001)	-0.055*** (0.001)	-0.055*** (0.001)
NDMI	-0.058*** (0.009)	-0.058*** (0.009)	0.119*** (0.010)	0.119*** (0.010)
Observations	1,901,934	1,901,934	2,399,998	2,399,998
R-squared	0.322	0.322	0.472	0.472
Pixel Fixed Effects	Yes	Yes	Yes	Yes
District Fixed Effects	Yes	Yes	Yes	Yes
Month Fixed Effects	Yes	Yes	Yes	Yes
Clustering	State-Location-Time	District-Location-Time	State-Location-Time	District-Location-Time

Robust standard errors in parentheses

*** p<0.01, ** p<0.05, * p<0.1

Table A10: Results with alternative clustering from Landsat 8. Clustering errors when the numbers of clusters is few is difficult. To address this, we leverage geographic coordinates to create degree-minute indicators. We then use this along with administrative categories like state and district along with time (month-year) to form clusters. This allows us to address correlation by location as well as serial correlation over time.

1.6 Main Result with log(NDVI) as outcome and percentage coefficients

	(1)	(2)	(3)	(4)
VARIABLES	Base Model	Full Model	Kharif	Rabi
1.treat#1.post	0.498*** (0.000)	0.750*** (0.000)	0.795*** (0.000)	0.620*** (0.000)
treat = 1	0.610*** (0.000)			
post = 1	-0.810*** (0.000)	-1.766*** (0.000)	-3.591*** (0.000)	-1.615*** (0.000)
NDMI		-10.448*** (0.001)	-14.995*** (0.002)	14.781*** (0.002)
Observations	5,731,856	5,731,856	1,901,932	2,399,998
R-squared	0.001	0.409	0.332	0.468
Pixel Fixed Effects	No	Yes	Yes	Yes
District Fixed Effects	No	Yes	Yes	Yes
Month Fixed Effects	No	Yes	Yes	Yes
Robust SE	No		Yes	Yes
Clustering		Yes		

Standard errors in parentheses

*** p<0.01, ** p<0.05, * p<0.1

Table A11: Table shows NDVI productivity change in percentage change terms. Original coefficients corrected by transformation into percentage terms since the specification has a log-transformed dependent variable and a dummy independent variable. Displayed coefficients $\approx (e^{\text{coef}} - 1) * 100$.

Table A14: Modis-250 Result with log(NDVI) as outcome and percentage coefficients

VARIABLES	(1) Base Model	(2) Full Model	(3) Kharif	(4) Rabi
1.treat#1.post	0.596*** (0.000)	0.371*** (0.000)	0.592*** (0.000)	0.519*** (0.000)
treat = 1	0.798*** (0.000)			
post = 1	-1.682*** (0.000)	-1.266*** (0.000)	-1.961*** (0.001)	-0.665*** (0.000)
NDMI		29.431*** (0.004)	30.817*** (0.006)	63.340*** (0.007)
Observations	6,398,014	6,313,911	1,994,840	2,399,400
R-squared	0.004	0.676	0.497	0.699
Pixel Fixed Effects	No	Yes	Yes	Yes
District Fixed Effects	No	Yes	Yes	Yes
Month Fixed Effects	No	Yes	Yes	Yes
Robust SE	No		Yes	Yes
Clustering		Yes		

Standard errors in parentheses

*** p<0.01, ** p<0.05, * p<0.1

Table A15: Table shows NDVI productivity change in percentage change terms. Original coefficients corrected by transformation into percentage terms. Displayed coefficients $\approx (e^{\text{coef}} - 1) * 100$.

1.7 NDVI to Yield Conversion

Conversion factor NDVI to Yield		
	(1)	(2)
VARIABLES	Kharif	Rabi
log_diff_ndvi_kharif	2.486** (1.161)	
log_diff_ndvi_rabi		1.458* (0.855)
(mean) rainfall	0.003 (0.003)	0.000 (0.002)
(mean) tmax	-0.247*** (0.067)	-0.224*** (0.046)
(mean) tmin	0.317*** (0.075)	0.206*** (0.046)
Observations	91	91
R-squared	0.758	0.882
State-Year Fixed Effects	Yes	Yes

Robust standard errors in parentheses

*** $p < 0.01$, ** $p < 0.05$, * $p < 0.1$

Table A16: Table shows an approximate conversion of NDVI productivity change to yield in percentage terms.

Table A5: Pixel Count by various landcover classes in Copernicus Global Land-Cover

Landcover Class	Number of Pixels
Unknown. No or not enough satellite data available	0
Shrubs	141491
Herbaceous Vegetation	57205
Cultivated Land/Agriculture	2733491
Urban/Built Up	46177
Bare	20677
Snow	0
Permanent Water Bodies	40916
Herbaceous Wetland	8878
Moss and Lichen	0
Closed Forest, Evergreen Needle Leaf	0
Closed Forest, Evergreen Broad Leaf	8464
Closed Forest,deciduous Needle Leaf	0
Closed Forest,deciduous Broad Leaf	777935
Closed Forest,Mixed	0
Closed Forest, not matching any of the other	62936
Open Forest, Evergreen Needle Leaf	0
Open Forest, Evergreen Broad Leaf	2707
Open Forest,deciduous Needle Leaf	0
Open Forest,deciduous Broad Leaf	112606
Open Forest,Mixed	0
Open Forest, not matching any of the other	234150
Oceans, seas. Can be either fresh or salt-water bodies	0
Total Population of Pixels	4247633

Table A12: Sentinel-2 Result with log(NDVI) as outcome and percentage coefficients

VARIABLES	(1) Base Model	(2) Full Model	(3) Kharif	(4) Rabi
1.treat#1.post	0.460*** (0.000)	0.462*** (0.000)	1.082*** (0.000)	0.419*** (0.000)
treat = 1	1.059*** (0.000)			
post = 1	-1.698*** (0.000)	-2.269*** (0.000)	-5.170*** (0.000)	-1.079*** (0.000)
NDMI		33.103*** (0.002)	30.045*** (0.004)	36.237*** (0.003)
Observations	2,325,267	2,301,325	599,625	1,187,668
R-squared	0.006	0.591	0.526	0.603
Pixel Fixed Effects	No	Yes	Yes	Yes
District Fixed Effects	No	Yes	Yes	Yes
Month Fixed Effects	No	Yes	Yes	Yes
Robust SE	No		Yes	Yes
Clustering		Yes		

Standard errors in parentheses

*** p<0.01, ** p<0.05, * p<0.1

Table A13: Table shows NDVI productivity change in percentage change terms. Original coefficients corrected by transformation into percentage terms. Displayed coefficients $\approx (e^{\text{coef}} - 1) * 100$.